Comprehensive analysis of TEAD inhibition in meningioma identifies MEK and mTOR inhibition as effective combination therapies against resistant lines.

Dylan J Keiser[1]*, Meghan S Buddy[1]*, Solmaz Mojarad-Jabali[1], Qing Li[1], Missia Kohler-Skinner[1,3], Abigail G Parrish[4], David Gillespie[1,2], David Nix[1], Sheri Holmen[1,5,6], Howard Colman[1,2], William Couldwell[2], Randy Jensen[1,2], Frank Szulzewsky[1,2,5]

1 Huntsman Cancer Institute, University of Utah, Salt Lake City, UT 84112, USA.

2 Department of Neurosurgery, Clinical Neurosciences Center, University of Utah, Salt Lake City, UT 84112, USA.

3 Department of Anatomic Pathology, University of Utah School of Medicine, Salt Lake City, UT 84112, USA.

4 Human Biology Division, Fred Hutchinson Cancer Center, Seattle, WA, 98109, USA.

5 Department of Oncological Sciences, University of Utah Health Sciences Center, Salt Lake City, Utah 84112, USA.

6 Department of Surgery, University of Utah Health Sciences Center, Salt Lake City, Utah 84112, USA.

* Contributed equally

Corresponding author:
Frank Szulzewsky
Department of Neurosurgery
Huntsman Cancer Institute
University of Utah
2000 Circle of Hope Dr.
Room 2713
Salt Lake City, UT 84112
Tel: 801-213-4217
Email: frank.szulzewsky@hsc.utah.edu

Abstract

Meningiomas are the most common primary central nervous system tumors in adults, posing a significant burden to society. Although a large percentage of lower-grade meningiomas are curable by surgery or radiation alone, high-grade and a subset of low-grade meningiomas demonstrate recurrences and complications from treatment. Systemic therapies for meningioma

remain ineffective, and no targeted treatments are approved. Despite the central role of YAP1/TAZ-TEAD signaling in NF2-deficient/mutant tumors, no studies have systematically examined TEAD inhibition across molecularly defined meningioma subtypes or investigated mechanisms of resistance in this disease. We have recently shown that YAP1/TAZ signaling is an oncogenic driver of meningioma. Here, using established and patient-derived meningioma cell lines, we demonstrate that genetic ablation of YAP1/TAZ suppresses growth in both NF2 mutant and NF2 wild type cell lines, establishing YAP1/TAZ-TEAD signaling as a shared oncogenic dependency. Pharmacologic TEAD inhibition suppressed growth of benign NF2 mutant and a subset of higher-grade NF2 mutant meningiomas, whereas NF2 wild type meningiomas were generally more resistant. RNA-Seq and Western Blot analysis identified compensatory activation of MEK-ERK, mTOR-S6, and FAK signaling in resistant lines exhibit. Importantly, co-targeting these pathways was able to overcome resistance to TEADi and was superior to MEK/mTOR/FAK inhibition alone. These studies provide a compelling proof-of-concept that TEADi represents a novel therapeutic vulnerability in meningioma and reveal adaptive signaling responses that can be therapeutically exploited.

Introduction

Meningiomas are the most common primary central nervous system (CNS) tumors in adults, with an incidence of 9.73 per 100,000 people per year, comprising 37.6% of all primary CNS tumors [1,2]. The incidence increases with age, with an incidence rate of 18.69 per 100,000 people per year in patients aged 40 and over [3]. Despite being the most common primary CNS tumor in adults, meningiomas have been significantly understudied compared to other CNS malignancies, such as glioblastoma. The majority of meningiomas are generally benign and curable by surgery alone, however, around 15-20% are of higher-grade, with a rising incidence [4,5]. Higher-grade meningiomas frequently show aggressive and invasive growth and recur even after multiple rounds of surgery and radiation and are ultimately fatal, highlighting the need for additional therapeutic options [6]. In addition, a significant number of meningiomas are often less accessible to surgery (such as skull base or optic nerve sheath meningiomas) due to their deep location and/or their frequent involvement of major blood vessels and cranial nerves, preventing complete resection and leading to recurrences and/or worsening symptoms [7].

Chemotherapeutic agents used for the treatment of other solid tumors, including cyclophosphamide, doxorubicin, temozolomide, and vincristine, have been largely ineffective in meningiomas [8-12]. The advance of high-throughput sequencing has led to the identification of clinically-relevant subtypes and molecular drivers of meningioma [13,14], however, although this has opened the door for a novel classification and diagnostic, it has so far not translated into effective novel targeted therapies. Targeted inhibitors, including FAK, PI3K, CDK4/6, and EZH2 inhibitors are currently undergoing clinical assessment and might show efficacy in a subset of patients [15-17]. Therefore, additional chemotherapeutic approaches are urgently needed for the treatment of meningiomas that are either inaccessible to surgery or for the management of hard-to-treat high-grade meningioma types that recur even after multiple rounds of surgery and radiotherapy.

Over the past two decades, large-scale genomic and epigenomic studies have reshaped the molecular taxonomy of meningioma. Recurrent somatic alterations include mutations in NF2, TRAF7, KLF4, AKT1, SMO, POLR2A, and BAP1, as well as chromosomal copy number changes and DNA methylation-based subgroups that more accurately predict clinical outcome than histology alone [13,14,18-21]. Among these alterations, inactivation of NF2 is the most frequent event, occurring in approximately 40–60% of sporadic meningiomas [14,19,22]. Furthermore, patients with neurofibromatosis type 2 also frequently develop multiple meningiomas [23]. Importantly, NF2 loss converges functionally on dysregulation of the Hippo signaling pathway and activation of the transcriptional co-activators YAP1 (Yes-associated protein 1) and TAZ (WWTR1) [24-26], positioning the YAP1/TAZ–TEAD axis as a central driver in a substantial subset of meningiomas.

The Hippo pathway is an evolutionarily conserved kinase cascade that regulates organ size, tissue homeostasis, regeneration, and stem cell behavior [27]. In its canonical configuration, upstream regulators including NF2 (Merlin), SAV1, and other polarity and cytoskeletal proteins promote activation of the MST1/2 kinases, which in turn phosphorylate and activate LATS1/2. Activated LATS kinases phosphorylate YAP1 and TAZ, resulting in their cytoplasmic retention, ubiquitin-mediated degradation, or functional inactivation [27]. When Hippo signaling is suppressed – such as through genetic loss of NF2 – YAP1 and TAZ accumulate in the nucleus. There, they bind members of the TEAD (TEA domain) family of transcription factors (TEAD1–4), which serve as the primary DNA-binding partners of YAP1/TAZ, and drive expression of genes involved in proliferation (e.g., CTGF, CYR61), survival, extracellular matrix remodeling, and stemness [28]. In many solid tumors, persistent YAP1/TAZ–TEAD activity promotes oncogenic transformation, tumor growth, metastasis, and therapeutic resistance.

We and others have detected increased YAP1/TAZ-TEAD activity (measured via the expression of YAP1/TAZ-TEAD target genes, such as CTGF and CYR61) in NF2 mutant (NF2mut) meningioma tumor tissues and/or cell lines compared to NF2 wild type (NF2wt) meningiomas [29-32]. Furthermore, the expression of a non-regulatable activated YAP1 variant (S127/397A-(2SA)-YAP1) induces transcriptional changes similar to functional NF2 loss in human neural stem cells and the intracranial expression of 2SA-YAP1 is sufficient to induce the formation of meningioma-like tumors in mice [32]. Lastly, recurrent YAP1 gene fusions (most commonly YAP1-MAML2) have been identified in a subset of pediatric NF2wt meningiomas [33]. The oncogenic functions of these YAP1 fusions fundamentally rely on their ability to exert de-regulated YAP activity and YAP1 fusion-positive human meningiomas resemble NF2mut meningiomas by both gene expression and DNA methylation-based classification [32-34]. These data suggest that the functional NF2 loss in meningiomas induces oncogenic YAP1/TAZ-TEAD activity and may be a therapeutic target in a subset of these tumors. However, while benign (low-grade) NF2mut meningiomas harbor few mutations in addition to functional NF2 loss, aggressive (high-grade) NF2mut meningiomas frequently harbor additional mutations and copy number losses [14,35,36]. The presence of these additional mutations may render aggressive-type NF2mut meningiomas less reliant on YAP1/TAZ-TEAD signaling. In line with this, we recently detected decreased levels of YAP1 activity (through the expression of direct YAP1 targets (e.g. CTGF)) in both bulk RNA-Seq samples as well as single-cell RNA-Seq samples of aggressive-type NF2mut meningiomas [30].

Given the prominent role of YAP1/TAZ–TEAD signaling in multiple cancers, therapeutic strategies targeting TEADs or the interaction between TEADs and YAP1/TAZ have been developed [37]. Structural insights into TEAD biology have revealed druggable vulnerabilities and current TEAD inhibitors generally either sterically block the interaction between TEAD and YAP1/TAZ (e.g. by occupying the TEAD Ω loop region) or by occupying the central hydrophobic pocket of TEAD blocking TEAD auto-palmitoylation [38-41]. Several pan-TEAD inhibitors (TEADi) have entered early-phase clinical trials (NCT04665206, NCT04857372) [42], particularly in tumors with NF2 loss or other modes of Hippo pathway dysregulation (e.g. Epithelioid Hemangioendotheliomas which frequently harbor WWTR1/TAZ or YAP1 gene fusions). However, their clinical development faces important challenges, including identification of robust predictive biomarkers of TEAD dependency, potential on-target toxicities given the role of YAP1/TAZ in normal tissue homeostasis and regeneration, and the emergence of adaptive resistance mechanisms or pathway bypass signaling. Despite these challenges, these agents provide proof-of-concept that TEAD is pharmacologically tractable and targeting YAP1/TAZ-TEAD signaling in specific tumor populations may have clinical benefit and raise the possibility of extending this strategy to molecularly selected meningioma patients.

Despite the prominent role of YAP1/TAZ-TEAD signaling in meningioma, the efficacy of TEADi has not been extensively studied in meningioma. Furthermore, pathways that may contribute to resistance-to-therapy need to be explored in order to inform effective combination therapies. Here, we explore the importance of YAP1/TAZ-TEAD signaling and the efficacy of TEADi, as well as potential combination therapies in multiple established and primary meningioma cell lines. First, we show that combined YAP1 and TAZ knockout results in highly significant growth reduction in all tested meningioma lines (including both NF2mut and NF2wt lines), suggesting that YAP1/TAZ-TEAD signaling is a central driver in meningiomas. Second, in vitro treatment of 22 established and clinical meningioma lines with four different TEAD inhibitors (IAG-933, MYF-03-176, GNE-7883, K-975) identified TEADi-sensitive and -resistant cell lines. While low-grade benign NF2mut cell lines were generally sensitive to TEADi, higher-grade NF2mut cell lines showed a more mixed behavior, and NF2wt cell lines were generally more resistant. RNA-Seq and Western Blot analysis of both TEADi-sensitive and -resistant lines identified an upregulation of MAPK and mTOR-S6 pathways in TEADi-resistant, but not -sensitive lines. Finally, the combination treatment of TEADi and mTORi or MEKi was able to overcome resistance to TEADi and yielded superior efficiency to either therapy alone. In summary, we establish YAP1/TAZ-TEAD signaling as a central driver in both NF2mut and NF2wt meningiomas and identify possible combination therapies that can overcome the resistance to TEADi.

Results

YAP1/TAZ expression is necessary for the growth of both NF2mut and NF2wt meningioma cells. To assess the importance of YAP1/TAZ-signaling for the growth of meningiomas, we used CRISPR-Cas9 gene editing to assess the effect of genetic ablation of YAP1/TAZ on the growth of meningioma cells. We tested the effect of combined YAP1+TAZ gene knockout and compared the growth and expression of YAP1/TAZ-TEAD target genes to

that of cells treated with CD8A control guides in three NF2mut (one low-grade (BenMen1) and two high-grade lines (KT21-MG1, CH157-MN)) and two NF2wt meningioma lines (IOMM-Lee, SAM). Successful gene knockout was confirmed by PCR/sanger sequencing (Suppl. Figure S1A). We observed a significant decrease in YAP1/TAZ-TEAD signaling, measured via the expression of CTGF, CYR61, ANKRD1, and AMOTL2 (Figure 1A; Suppl. Figure S1B). We performed live-cell imaging to analyze the impact of YAP1/TAZ double knockout on cell growth. We observed an almost complete inhibition of growth upon YAP1 and TAZ double knockout in the two of the three NF2mut cell lines (BenMen1, KT21-MG1). The cell confluence of BenMen1 and KT21-MG1 cells harboring a YAP1+TAZ double knockout did not significantly increase compared to t = 0 (1.075±0.08-fold increase (padj = 1) and 1.32±0.41-fold increase (padj = 0.98), respectively) (Figure 1B). We also observed a highly significant growth reduction for CH-157MN and the two NF2wt cell lines (IOMM-Lee, SAM) upon co-deletion of YAP1 and TAZ (Figure 1B), however, these lines still were able to significantly grow (1.37±0.04-fold increase (padj < 0.0001), 5.72±1.56-fold increase (padj < 0.0001), and 3.98±0.88-fold increase (padj = 0.01), respectively). These results suggest that YAP1/TAZ-TEAD signaling is involved in the growth of meningioma cells (including high-grade NF2mut and NF2wt subtypes) and therefore an attractive therapeutic target. However, while a subset of cells stops growing almost completely upon loss of YAP1/TAZ-TEAD signaling, other cell lines (most prominently NF2wt cells) are able to partially overcome this impact.

TEADi shows significant efficacy against benign and a subset of high-grade NF2 mutant meningioma cell lines. We collected 22 human meningioma cell lines, including four established lines (Ben-Men-1, KT21-MG1, CH-157MN, IOMM-Lee) and 17 primary lines, including both NF2mut and wild type cell lines. NF2/Merlin status was assessed via Western Blot staining (Suppl. Figure S2A). We then assessed the efficacy of four TEAD inhibitors (MYF-03-176, IAG-933, K-975, GNE-7883; doses of 1, 10, 50, 100, 200, 500, 1000, 2000, and 5000 nM, 0.1% DMSO as control)[38-41] via live-cell imaging, followed by CellTiter-Glo viability assays and determined absolute IC_{50} values for each inhibitor and cell line (n = 3 per cell line and inhibitor; Figure 2A-C; Suppl. Figure S2B-F). Cells were cultured until the DMSO control reached a confluency of >80 percent. A specific cell line was deemed sensitive if the absolute IC_{50} for a specific TEAD inhibitor was below 250 nM for IAG-933 treatment (determined by Cell Titer-Glo). While low-grade benign NF2mut cell lines were generally sensitive to TEADi, we identified both sensitive and resistant higher-grade NF2mut cell lines, while NF2wt cell lines were generally more resistant to TEADi treatment (Table 1). In general, IAG-933 and MYF-03-176 showed the highest efficacy in most cell lines (Figure 2A-C; Suppl. Figure S2B-F). Absolute IC_{50} values for IAG-933 ranged from 40-210 nM in low-grade NF2mut lines, but were as high as 1500 nM in NF2wt lines. By contrast, IC_{50} values for MYF-03-176 ranged from 76 nM-500 nM in low-grade NF2mut lines, but exceeded 5000 nM in NF2wt cell lines. In TEADi-sensitive lines both IAG-933 and MYF-03-176 showed comparable efficacies, whereas GNE-7883 and K-975 showed a lower efficacy but were still able to lead to a significant growth reduction. By contrast, in TEADi-resistant lines all inhibitors displayed significantly lower efficacies. However, while IAG-933, and to a lesser degree MYF-03-176, were still able to induce a significant growth reduction at higher concentrations, GNE-7883 and K-975 were frequently unable to exert any effect on the growth of resistant lines.

We treated four resistant and six sensitive cell lines with the four TEAD inhibitors (IAG-933 and MYF-03-176 (500 nM), GNE-7883 (5000 nM), K-975 (1000 nM)) for 72 hours and isolated total RNA (n = 3 per cell line and inhibitor). We detected a significant downregulation of canonical YAP1/TAZ targets (CTGF, CYR61, ANKRD1, AMOTL2) upon TEADi treatment via qRT-PCR in all TEADi-treated cell lines (Figure 2D; Suppl. Figure 2G), regardless of the NF2 status or sensitivity/resistance to TEADi. In TEAD-sensitive cell lines, the ability of a specific inhibitor correlated with the degree of the downregulation of YAP1/TAZ-TEAD targets, e.g. IAG-933 and to a lesser degree MYF-03-176 resulted in the most significant decrease of target gene expression. Surprisingly, TEAD-resistant cell lines frequently displayed a larger degree of downregulation of YAP1/TAZ-TEAD target genes, suggesting that the ability of TEADi-resistant lines is not caused by the inability of TEADi to affect the expression of specific YAP1/TAZ-TEAD targets, but rather the presence of additional mitogenic pathways.

These results suggest that multiple subtypes of meningioma are reliant on YAP1/TAZ-TEAD signaling – further exemplified by the fact that YAP1/TAZ double knockout led to a growth arrest even in TEADi-resistant lines and that high TEADi concentrations can inhibit also the growth of these TEADi-resistant lines. However, while TEADi-sensitive lines are already responsive to lower TEADi doses, TEADi-resistant cells are not, potentially caused by the presence of other mitogenic pathways that can compensate to a degree.

TEADi treatment results in a downregulation of YAP1/TAZ-TEAD signaling in both TEADi-sensitive and -resistant cell lines. To analyze the response of meningioma cells to TEADi in more detail, we treated six meningioma cell lines (four NF2mut and two NF2 wild type lines) with DMSO or two different TEAD inhibitors (IAG-933 and MYF-03-176, 500 nM each) for 72 hours, isolated total RNA, and performed RNA-Seq (n = 3 per condition and cell line). We included three TEADi-sensitive (BenMen1 and BrMen (both low-grade NF2mut), KT21-MG1 (high-grade NF2mut)) and three TEADi-resistant lines (CH157-MN (high-grade NF2mut), IOMM-Lee and SAM (both NF2wt). Differential gene expression analysis followed by Principal Component Analysis (PCA) and hierarchical clustering of the DMSO-treated conditions revealed a clustering broadly along the lines of TEADi-sensitive cell lines (BenMen1, BrMen, KT21-MG1) and TEADi-resistant lines (CH157-MN, IOMM-LEE, SAM) (Figure 3A). TEADi-treated conditions remained in these clusters, suggesting that the overall cell line state is dominant over the transcriptional changes induced by TEADi treatment (Figure 3B). However, TEADi-treated cells displayed a significant shift away from DMSO-treated cells that was consistent across all cell lines. This degree of this shift correlated with the degree of inhibition of YAP1/TAZ-TEAD signaling and was greater for IAG-933-treated vs MYF-03-176-treated cells (Figure 3B-D, Suppl. Figure S3A).

Treatment with both IAG-933 and MYF-03-176 resulted in highly significant changes of gene expression in all six cell lines (adjusted p-value (padj) < 0.05; fold change (FC) > 1.5) (Suppl. Figure S3B). The gene expression changes induced by TEADi (compared to DMSO) significantly overlapped between IAG-933 and MYF-03-176-treated samples, although IAG-933 resulted in a higher number of deregulated genes and a significantly stronger degree of deregulation (Figure 3E-F, Suppl. Figure S3B-E). In addition, transcriptomic changes induced by the TEADi treatment showed highly significant overlaps between the different cell lines (including both resistant and sensitive lines), suggesting that TEADi treatment induces similar

transcriptomic changes in both sensitive and resistant lines (Suppl. Figure S3F). Lastly, the differentially expressed genes were significantly enriched for YAP1/TAZ-TEAD target genes, suggesting that a significant portion of the TEADi-induced transcriptomic changes are mediated by on-target inhibition of YAP1/TAZ-TEAD signaling (Suppl. Table S1). In summary, TEADi treatment induces highly significant changes in the transcriptome of meningioma cells. These changes were highly similar between sensitive and resistant lines and the degree of gene regulation correlates with inhibitor efficacy.

TEADi induces MEK-ERK and mTOR-S6 (but not PI3K-AKT) signaling in TEADi-resistant cell lines. KEGG pathway analysis revealed a significant enrichment of terms related to “DNA replication” and “Cell Cycle” (Suppl. Table S2). In addition, we observed a significant enrichment of terms related to RTK-PI3K, RTK-Ras-PI3K, RTK-Ras-ERK, FAK, RhoA, BMP, JAK-Stat, and Wnt signaling pathways for multiple cell lines. To confirm the differential regulation of the PI3K and MAPK pathways upon TEADi-treatment, we treated seven TEAD-sensitive (BenMen1, BrMen, KT21-MG1, ARC, FAS, MUL, patient tumor 16) and three TEADi-resistant lines (IOMM-Lee, GAR, SAM) with IAG-933 and MYF-03-176 (500 nM each) for 72 hours, isolated total protein, and performed Western Blots for phospho and total levels of AKT, S6, and ERK (Figure 4A, Suppl. Figure S4A). We observed a significant decrease in phospho-S6 levels in all TEADi-sensitive lines upon treatment with both IAG-933 and MYF-03-176, with the former showing a greater degree of regulation. In addition, we also observed a significant decrease in phospho-ERK levels in most TEADi-sensitive cell lines upon treatment. By contrast, we observed a significant increase in phospho-S6 levels in all TEADi-resistant lines upon treatment. The degree of increase was generally higher in IAG-933 treated cells, compared to MYF-03-176. Similarly, phospho-ERK levels were also increased in most TEADi-resistant lines upon treatment. Since we observed a decreased activation of AKT in most TEADi-sensitive and -resistant upon treatment, the activation of mTOR-S6 may be independent of PI3K-AKT signaling and achieved via alternative pathways, such as the direct activation of p90-ribosomal S6 kinase (RSK) or inactivation of Tuberous sclerosis-2 (TSC-2). In summary, we identified diametrically opposed activation of MAPK and mTOR-S6 pathways in TEADi-sensitive and -resistant meningioma lines upon TEADi treatment.

Co-targeting MAPK and mTOR-S6 signaling is able to overcome resistance to TEADi. Since we observed a significant upregulation of MEK-ERK and mTOR-S6 pathways upon TEADi treatment of TEADi resistant meningioma cell lines, we next assessed whether cotreatment of resistant cells with MEK (MEKi (trametinib)), PI3K (PI3Ki (pictilisib)), or mTOR inhibitors (mTORi (torin-2)) can increase the efficacy of TEADi in these cells. We treated TEADi-sensitive and -resistant cell lines with either IAG-933 (200 nM (sensitive lines), 500 nM (resistant lines)), MEKi (1, 5, 10 nM), or mTORi (5, 10, 20 nM), alone or in combination. Treatment efficacy was measured via live cell imaging and endpoint Cell Titer-Glo measurements. While co-treatment with MEKi or mTORi did not significantly increase the efficacy of TEADi (at 200 nM) in TEADi-sensitive cell lines, it was able to significantly increase the efficacy of TEADi in all tested resistant cell lines, even at low MEKi (1 nM) or mTORi (5 nM) concentrations (Figure 5A-B, Suppl. Figure S5A-B). Importantly, the combination of TEADi and MEKi or mTORi showed a significantly greater inhibition of growth and cell viability than MEKi or mTORi alone, or the combination of MEKi and mTORi (without TEADi) in all tested TEADi-

resistant cell lines (Figure 5A-B, Suppl. Figure S5A-B). Treatment with a PI3K inhibitor (Pictilisib, 50-100 nM) did not show any significant efficacy (Figure 5A), which is in accordance with our finding that phospho-AKT levels were decreased upon TEADi treatment even in TEADi-resistant cell lines.

We performed additional in vitro treatment experiments followed by CellTiter-Glo viability readout after 5 days of treatment, and used SynergyFinder3.0 to identify synergistic drug effects between TEADi and MEKi or mTORi in TEADi-resistant and -sensitive cell lines. We treated five TEADi-sensitive (ARC, BenMen1, KT21-MG1, patient 5, patient 16), and six TEADi-resistant (IOMM-Lee, CH157-MN1, SAM, GAB, GAR, patient 12) cell lines with increasing concentrations of IAG-933 (25, 75, 225, 675, 2025 nM) and trametinib or torin-2 (0.11, 0.33, 1, 3, 5, 9, 27 nM for both). For TEADi-sensitive cell lines, we only observed synergistic effects between IAG-933 and trametinib at low IAG-933 concentrations (25 and 75 nM), but not at higher concentrations (Figure 5C, Suppl. Figure S5C). By contrast, in TEADi-resistant cell lines we observed synergistic effects with as low as 1 nM of trametinib treatment (Figure 5C, Suppl. Figure S5C). Similarly, cotreatment with torin-2 and IAG-933 in TEADi-sensitive cells (ARC, KT21-MG1, patient 5, patient 16) also only resulted in synergistic effects at low IAG-933 concentrations (25 and 75 nM), whereas cotreatment of TEADi-resistant cells (IOMM-Lee, CH157-MN1, GAB, GAR, patient 12) revealed synergistic effects for torin-2 concentrations of 1 nM and higher (Figure 5C, Suppl. Figure S5D).

We treated TEADi-resistant IOMM-Lee (NF2wt) and CH157-MN (high-grade NF2mut) cells with IAG-933 (500 nM), trametinib (10 nM), torin-2 (10 nM), or pictilisib (50 nM) and combinations thereof for 72 hours and subsequently isolated whole protein lysates. We performed Western Blots for phospho-AKT, phopsho-S6, and phospho-ERK to assess on-target drug efficacies and observed inhibitor-specific inhibition of these pathways. In IOMM-Lee cells, cotreatment of IAG-933 and trametinib resulted both in a reduction of phospho-ERK and phsopho-S6 levels, demonstrating the direct link between MEK-ERK signaling and PI3K-AKT-independent mTOR activation in these cells upon TEADi treatment (Figure 5D). Similar observations were made in CH-157MN cells (Suppl. Figure S5E).

In summary, combination treatments of IAG-933 and MEK or mTOR inhibitors show significant efficacy in overcoming the short-term resistance to TEADi in TEADi-resistant meningioma cell lines. Importantly, the combination of TEADi with MEK or mTOR inhibitors was superior to either inhibitor alone and was also superior to the combination of MEKi and mTORi.

Additional FDA-approved mTOR inhibitors show a similar beneficial effect in combination with TEADi. While trametinib has been approved by the FDA for the clinical application in multiple clinical settings, including the use in meningioma and other CNS tumors (such as low-grade glioma in combination with the Raf inhibitor dabrafenib), torin-2 is not an FDA-approved inhibitor and is not currently being assessed in clinical trials, despite high efficacy in multiple preclinical studies [43]. To this end, we assessed the ability of additional FDA-approved mTOR inhibitors (vistusertib, everolimus, rapamycin, sapanisertib, and torin-2 as a positive control) to significantly enhance the efficacy of TEADi in TEADi-resistant meningioma cell lines. We treated TEADi-resistant CH-157MN meningioma cells with IAG-933 (200 nM), mTOR inhibitors (1, 3, 5, 10, 20, 50 nM), or a combination of IAG-933 and mTORi. As previously

observed for torin-2, single-agent treatment of CH-157MN cells with the different mTOR inhibitors did not result in a significant growth arrest or reduction in viability (Suppl. Figure S5F), apart from 20 and 50 nM doses of torin-2 and sapanisertib (data not shown). By contrast, co-treatment of CH157-MN cells with IAG-933 and the different mTOR inhibitors showed a significant growth reduction beyond the effect of single-agent IAG-933 or single-agent mTORi (Figure 5E, Suppl. Figure S5F). All tested FDA-approved mTOR inhibitors, apart from vistusertib, displayed a similar ability to overcome TEADi resistance compared to torin-2 ($p < 0.0001$ (vistusertib vs torin-2); $p = 0.17$ (everolimus vs torin-2); $p = 0.6$ (rapamycin vs torin-2); $p = 0.56$ (sapanisertib vs torin-2)). In summary, cotreatment with the FDA-approved mTOR inhibitors everolimus, rapamycin, and sapanisertib is able to significantly increase the efficacy of TEADi against TEADi-resistant meningioma cell lines in a similar manner to torin-2.

Combined TEAD and FAK inhibition exert additive inhibitory effects in a subset of meningioma cell lines. Since the KEGG terms of multiple cell lines analyzed by RNA-Seq also showed an enrichment of Focal Adhesion signaling in TEADi-treated cell conditions, we assessed the efficacy of a FAK inhibitor (TAE226, 500 nM) alone or in combination with IAG-933 (100 nM for BenMen1 and KT21-MG1; 500 nM for the remaining cell lines) in nine cell lines, including TEADi-sensitive (BenMen1, KT21-MG1) and -resistant cell lines (CH157-MN, IOMM-Lee, SAM, Patient 6, 8, 9, 12), and assessed the impact on cell viability via CellTiter-Glo. Patient cell lines 8 and 9 were only tested for single-agent TAE226. Single-agent TAE226 treatment was able to significantly inhibit the viability and growth of five out of nine cell lines (BenMen1 and KT21-MG1 (both TEADi-sensitive NF2mut cell lines); patient tumors 6, 9, and 12), but was generally less effective compared to IAG-933 treatment (Figure 5F, Suppl. Figure S5G). Cotreatment of IAG-933 and TAE226 was able to further significantly reduce the viability compared to the single-agent IAG-933 conditions in three out of seven cell lines (BenMen1, KT21-MG1, SAM cells). CH-157-MN and patient tumor 6 cells showed a non-significant trend towards reduced viability in TAE226+IAG-933 co-treated cells, compared to single-agent IAG-933-treated cells ($p = 0.08$ and 0.07, respectively). In summary, cotreatment of TEADi with FAK inhibitors is beneficial for a subset of meningioma cell lines, including both TEADi-sensitive and -resistant lines. Although the combination with FAK inhibition is less potent compared to MEKi and mTORi cotreatment in TEADi-resistant lines.

Discussion

Although the majority of meningiomas are benign and curable by surgery alone, a significant proportion are of higher grade, display aggressive growth behavior, and invade into the brain and recur even after multiple surgeries. In addition, a significant portion of meningiomas grows in locations that are difficult to access via surgery due to their deep location and/or their frequent involvement of major blood vessels and cranial nerves (such as the skull base and optic nerves), preventing complete resection and leading to recurrences and/or worsening symptoms even in low-grade tumors. Chemotherapeutic drugs commonly used to treat other solid tumors—such as cyclophosphamide, doxorubicin, temozolomide, and vincristine—have generally shown limited effectiveness in meningiomas [8-12]. Meanwhile, several targeted therapies, including inhibitors of FAK, PI3K, CDK4/6, and EZH2, are currently being evaluated in clinical trials and may demonstrate benefit in a subset of patients [17].

The clear biological convergence of multiple molecular meningioma subtypes on YAP1/TAZ–TEAD–dependent signaling serves as a strong argument for the use of TEAD inhibitors in meningioma. NF2 loss, the most common genetic event in meningioma, disrupts Hippo pathway regulation and promotes deregulated YAP1/TAZ activity, while recurrent YAP1 fusions in NF2wt tumors produce constitutively active TEAD-driven transcriptional programs. This convergence suggests that TEAD represents a shared downstream vulnerability across genetically distinct but mechanistically related meningioma subgroups and providing a strong rational for inhibiting the YAP1/TAZ-TEAD complex in meningioma. 1) Our experimental data suggests that both NF2mut and wild type meningioma cells rely on YAP1/TAZ-TEAD signaling for their growth, since we observed a highly significant reduction in cell growth upon combined CRISPR-Cas9-mediated genetic perturbation of YAP1 and TAZ. 2) We observed that treatment with TEAD inhibitors by itself was sufficient to significantly reduce the growth of multiple “TEADi-sensitive” meningioma lines (predominantly lower-grade NF2mut as well as a subset of high-grade NF2mut tumors). 3) While we observed that NF2wt meningioma cells are generally more resistant to TEADi, we found that resistant cells respond to TEADi upon targeting compensatory pathways with MEK or mTOR inhibitors. Importantly, the combination of TEADi with MEK or mTOR inhibitors was superior to either inhibitor alone and was also superior to the combination of MEKi and mTORi, suggesting that TEADi sensitizes these cells to MEK/mTOR inhibition. Synergistic effects between TEADi and MEKi/mTORi were observed at concentrations as low as 1 nM for both the MEK inhibitor trametinib and the mTOR inhibitor torin-2. We could furthermore show that additional, FDA-approved mTOR inhibitors exert a similar ability to significantly increase the efficacy of TEADi in resistant cells. In TEADi-sensitive meningioma cell lines, combination therapies of TEADi and MEKi/mTORi only show synergistic effects at lower IAG-933 doses. The combination of TEADi and MEKi/mTORi in TEADi-sensitive meningiomas may however still be beneficial for the use of other TEAD inhibitors that display lower efficacy compared to IAG-933. In addition, although the blood brain barrier is generally not an issue for drug delivery into meningiomas, limited in vivo bioavailability of TEAD inhibitors may still reduce drug delivery into the tumor tissue.

In addition to MEK and mTOR inhibition, we also identified FAK inhibition as an additional option for cotreatment. Although not as effective as MEKi/mTORi, cotreatment with the FAK inhibitor TAE226 was able to significantly further increase the efficacy of TEADi in around half of the tested cell lines. RNA-Seq analysis of TEADi-treated meningioma cells identified additional enriched pathways, such as WNT, RhoA, Interleukin2/6-Jak-STAT, and IFN signaling pathways, and future experimentation will be needed to ascertain the importance of these pathways in the resistance to TEADi. Our results suggest that the activation of the mTOR-S6 pathway in TEADi-resistant lines upon TEADi treatment may occur via the ERK pathway, rather than via the PI3K-AKT axis. ERK-dependent mTOR activation can occur via the ERK1/2-mediated phosphorylation of Raptor or TSC2 [44,45]. However, the factors that contribute to the activation of MAPK signaling in TEADi-resistant cells upon TEADi treatment are still unclear and will need to be explored in future experimentation.

We observed significant differences in the efficacy of the four tested TEAD inhibitors (IAG-933, MYF-03-176, GNE-7883, K-975) to inhibit the growth of both TEADi-sensitive and -resistant meningioma cell lines. This was in part due to the higher on-target efficacy of IAG-933

and MYF-03-176, exemplified by their significantly stronger ability to down-regulate YAP1/TAZ-TEAD target genes. However, while all four inhibitors were able to inhibit the growth of TEADi-sensitive cell lines to a degree, only IAG-933 was still able to partially inhibit the growth of TEADi-resistant lines albeit at higher concentration. It was puzzling why MYF-03-176 was able to inhibit the growth of TEADi-sensitive lines with a similar efficacy as IAG-933, but performed significantly worse than IAG-933 against resistant lines. Of note, IAG-933 and MYF-03-176 have reported different affinities to the four different TEAD proteins, with MYF-03-176 showing a higher affinity to TEAD1&3 [40]. The four inhibitors inhibit YAP1/TAZ-TEAD signaling via different mechanisms. MYF-03-176 and K-975 target the TEAD palmitate pocket and prevent auto-palmitoylation, GNE-7883 binds to the lipid pocket of TEADs, whereas IAG-933 binds to and blocks the TEAD Ω-loop that is necessary for YAP1/TAZ-TEAD interaction. Future experiments will be necessary to determine whether a specific type of TEAD inhibitor is more effective against specific tumor and meningioma subsets.

All of our treatment experiments were limited to short-term treatments (1 week maximum) and the resistance to long-term TEADi treatment in meningiomas will need to be explored. Studies in NF2mut mesothelioma cell lines have identified increased AP-1 (activator protein-1) transcription, MYC and HGF overexpression, as well as upregulation of MAPK (NF1 loss) and JAK-STAT (SOCS3 loss) as potential causes for acquired resistance to TEADi (K-975, GNE-7883, MRK-A) [39,46-48]. A direct combination with MEK inhibitors may be able to overcome or prevent some of these resistance mechanisms from occurring.

Several TEAD inhibitors are currently or have previously been under clinical investigation. Despite their potential benefit in NF2mut/YAP1-TAZ-driven tumors (such as meningioma), TEAD inhibitors have encountered several hurdles in clinical trials. Both IAG-933 (NCT04857372, Novartis) and VT3989 (NCT04665206, Vivace Therapeutics) have reported limited clinical efficacy in their respective patient population [42,49]. Co-targeted of TEADi with MEKi/mTORi may yield increased clinical efficacy. Furthermore, TEADi has recently been linked to kidney toxicity [50], which could make the current generation of TEADi unfeasible for clinical use. However, the goal of this study is a proof-of-concept to show that TEADi is able to reduce the growth and viability of meningiomas cells. Future research could determine what causes this toxicity and lead to new next-generation inhibitors (that are more selective to a specific TEAD variant) or ultrasound-activated burst-release nanoparticles could be utilized to deliver TEADi more locally.

In summary, our results establish YAP1/TAZ-TEAD signaling as a prominent oncogenic driver in meningioma and serve as a proof-of-concept and strong rational for the clinical application of TAD inhibitors in meningioma. We furthermore explore pathways that contribute to the resistance to TEADi and identify MEK, mTOR, and FAK inhibition as effective combination therapies.

Methods

Cell lines

BenMen1 cells were purchased from DSMZ (Deutsche Sammlung von Mikroorganismen und Zellkulturen GmbH). The KT21-MG1, CH-157MN, and IOMM-Lee cell lines were kind gifts of Dr. Jonathan Chernoff (Fox Chase Cancer Center), Dr. Yancey Gillespie (University of Alabama School of Medicine, Birmingham, Alabama), and Dr. Ian McCutcheon (University of Texas, M.D. Anderson Cancer Center, Houston, Texas), respectively. GAR, GAB, SAM, NOR, FAS, MUL, ARC, PRO, BrMen, and GRA cell lines were previously collected by Dr. Randy Jensen [51]. Primary patient cell lines were established from patient samples collected under the Huntsman Cancer Institute Total Cancer Care (TCC) IRB (IRB 89989). Tumor tissues from which primary tumor lines were established were graded by a board-certified neuropathologist.

BenMen1 cells were grown in DMEM (Thermo Fisher Scientific 11995065), 20% FBS (Thermo Fisher Scientific A5670701), 1% Pen/Strep). All other cell lines were grown in 10% FBS. For primary cell lines established from primary patient samples, tumor tissue was mechanically dissociated into small pieces, and cultured in DMEM 10% FSB 1% Pen/Strep.

In vitro growth assays

500-2000 cells per well (depending on the cell line and cell size) were seeded into 96 well plates in their respective media. 24 hours after seeding, 2x inhibitor concentrations were added into the wells to achieve a 1x inhibitor concentration. Appropriate DMSO-only concentrations were used as controls. Each condition was set up in triplicates. Cells were then incubated for 5-7 days (until the DMSO condition reach >80 percent confluency). Live cell imaging was performed using an Incucyte S3 Live-Cell Analysis System with images being acquired every 2 hours. Endpoint viability was measured using the CellTiter-Glo 2.0 Cell Viability Assay (Promega G9241) according to the manufacturer's instructions. Luminescence was detected using a Microplate Luminometer. For 2-way synergy testing, inhibitors were plated in unicates with concentrations ranging from 25 to 2025 nM (IAG-933) or 0.111 to 27 nM (trametinib, torin-2). Endpoint viability was measured using the CellTiter-Glo 2.0 Cell Viability Assay as described above and 2-way inhibitor synergies were calculated using SynergyFinder 3.0 [52].

Western Blot Analysis

For analysis of downstream pathway activation, cells were seeded into 6 or 12 wells, and incubated with appropriate inhibitor concentrations for 72 hours. Cells were cultured in media containing 0.5% FBS 24 hours prior to and during inhibitor treatment. Cells were incubated with either TEADi (IAG-933, MYF-03-176, 500 nM each), MEKi (trametinib 10 nM), mTORi (torin-2, 10 nM), or PI3Ki (pictilisib, 50 nM). Cells were cultured, lysed, and processed for western blotting by standard methods. Proteins were resolved by SDS/PAGE (NuPAGE 10% Bis/Tris; LifeTech) according to XCell Sure Lock Mini-Cell guidelines, blocked with 5% milk/TBST and probed with specified antibodies overnight at 4°C in 5% BSA/TBST. After three TBST rinses, species-specific secondary antibodies were added in 5% milk/TBST. Blots were rinsed three times with TBST before being developed with Amersham ECL Western Blotting Detection Reagents (GE Healthcare). For a list of antibodies used see Suppl. Table S3A.

Inhibitors

Inhibitors were purchased from MedChemExpress (MCE), Sigma-Aldrich (SA), or SelleckChem (SC) (IAG-933 (MCE HY-153811; SC E1490); MYF-03-176 (SA SML3686-5MG); GNE-7883 (MCE HY-147214), K-975 (MCE HY-138565); trametinib (MCE HY-10999); torin-2 (MCE HY-13002); pictilisib (MCE HY-50094); vistusertib (MCE HY-15247); everolimus (MCE HY-10218); rapamycin (MCE HY-10219); sapanisertib (MCE HY-13328).

CRISPR-Cas9 gene editing

Cells were transiently transfected with ribonucleoprotein complexes composed of chemically synthesized 2′-*O*-methyl-3′phosphorothioate-modified single guide RNAs (sgRNAs) and purified Cas9 protein using an Amaxa 4D nucleofector as previously described [53]. Two guides each were used for YAP1 and WWTR1 (TAZ). A guide RNA targeting CD8A served as a control. Guide sequences are listed in Suppl. Table S3B. Successful gene editing was assessed 96 hours post nucleofection via targeted PCR followed by Sanger Sequencing and subsequent Synthego Inference of CRISPR Edits (ICE) analysis. Primer sequences for targeted PCRs are listed in Suppl. Table S3C Functional impact of YAP1/TAZ codeletion was assessed via qRT-PCR for YAP1/TAZ-TEAD target gene expression and live-cell imaging.

RNA Isolation, PCR, and RNA Sequencing

For analysis of YAP1/TAZ-TEAD target gene regulation upon TEADi treatment, cell lines were seeded into 6 well plates and treated with TEADi for 72 hours (IAG-933 (500 nM, MYF-03-176 (500 nM), GNE-7883 (5000 nM), K-975 (1000 nM)). For analysis of YAP1/TAZ-TEAD target gene regulation upon CRISPR-Cas9-mediated genetic ablation of YAP1/TAZ, cells were seeded into 6 well plates 48 hours after CRISPR-Cas9 gene editing and RNA was isolated 48 hours later. RNA was extracted using the Qiagen RNeasy Mini Kit according to the manufacturer's instructions. Genomic DNA was removed by on-column DNase digestion. RNA concentration was measured with a Qubit RNA BR Assay Kit (Fisher Scientific #Q10211). RNA quality was evaluated with an Agilent Technologies RNA ScreenTape Assay (5067-5576 and 5067-5577). Poly(A) RNA was purified from total RNA samples (10-500 ng) using the NEBNext Poly(A) mRNA Magnetic Isolation Module (E7490). Stranded RNA sequencing libraries were prepared as described using the NEBNext Ultra II Directional RNA Library Prep Kit for Illumina (E7760L). Purified libraries were qualified on an Agilent Technologies 4150 TapeStation using a D1000 ScreenTape assay (cat# 5067-5582 and 5067-5583). The molarity of adapter-modified molecules was defined by quantitative PCR using the Kapa Biosystems Kapa Library Quant Kit (cat#KK4824). Individual libraries were normalized to 5 nM in preparation for Illumina sequence analysis. Sequencing libraries were chemically denatured in preparation for sequencing. Following transfer of the denatured samples to an Illumina NovaSeq X instrument, a 151 x 151 cycle paired end sequence run was performed using a NovaSeq X Series 25B Reagent Kit (20104706). For quantitative real-time PCR, RNA was transcribed into cDNA using the

SuperScript III kit. PCR experiments were carried out on a Bio-Rad Flex Real-Time PCR System. For primer sequences see Suppl. Table 3C.

Bioinformatic Analysis

RNA-seq reads (151 × 151 bp paired-end) were adapter-trimmed with cutadapt and optical duplicates removed with BBMap/Clumpify. Reads were aligned to the GRCh38 reference from Ensembl Release 112 using STAR v2.7.9a and gene-level counts were generated with featureCounts v1.6.3. Downstream analyses were performed in R using DESeq2 (v1.42.1); low-count features (≤5 reads) were filtered prior to testing, and regularized-log (rlog) values were used for visualization. Differential expression was defined at FDR < 0.05 and |log2 fold change| > 0.585 (≈1.5×). All overlap, union and Venn analyses were performed at the Ensembl gene-ID level (version suffixes removed) to avoid symbol ambiguities. Gene-set enrichment was assessed by Fisher's exact tests and ranked GSEA against MSigDB collections; multiple testing correction was applied (FDR).

Statistical Analysis

All statistical analyses were conducted using GraphPad Prism 10 (GraphPad software Inc.). Statistical differences between 2 populations were calculated by unpaired t test (2-tailed). For multiple populations' comparison, one-way or two-way ANOVA with Turkey's multiple-comparisons test was used. $p < 0.05$ was considered statistically significant. 2-way inhibitor synergies were calculated using SynergyFinder 3.0 [52].

Data Availability

The data that support the findings of this study are included with the manuscript and supplemental data files and are also available from the corresponding author upon reasonable request. RNA-Seq data from human meningioma cells expressing treated with either DMSO, IAG-933, or MYF-03-176 can be accessed at the GEO database at GSEXXXXXX.

Acknowledgments

We thank Anna Spangler-Temby for continued administrative assistance. We thank Dr. Martin McMahon for insightful discussions. Funding for this study was provided by the University of Utah Department of Neurosurgery and Huntsman Cancer Institute Start-up funds (FS). We acknowledge support from Zaily Connell and Brian Dalley from the High-Throughput Genomics and HCI's National Cancer Institute Cancer Center Support Grant P30CA042014.

Author contributions

R.J. and F.S. conceived the study. D.K., M.B., S.M.J., A.G.P., and D.G. performed the experiments. D.K., M.B., S.M.J., Q.L., M.K.S., and F.S. analyzed the data. F.S. and S.H. wrote the manuscript. Q.L. and F.S. reviewed and edited the manuscript. W.C., R.J., and F.S. acquired the funding. D.N., H.C., W.C., R.J., and F.S. supervised the study. All authors read, reviewed, and approved the manuscript.

Figure and Table legends

Table 1 - Overview of different meningioma cell lines and the absolute IC_{50} values of the four TEAD inhibitors tested.

Figure 1: Combined loss of YAP1 and TAZ (WWTR1) significantly reduces the growth of both NF2 mutant and NF2 wild type meningioma cells. A) Expression of the YAP1/TAZ-TEAD target gene CTGF in benign NF2mut (BenMen1 (n = 10 each)), aggressive high-grade NF2mut (KT21-MG1 (n = 3 each), CH-157MN (n = 3 each)), and NF2wt (IOMM-Lee (n = 14 each), SAM (n = 3 each)) meningioma cell lines upon CRISPR-Cas9-mediated inactivation of either CD8A (control) or combined inactivation of YAP1 and TAZ (WWTR1). B) Cell growth measured by live-cell imaging of benign NF2mut (BenMen1 (n = 5 each)), aggressive high-grade NF2mut (KT21-MG1 (n = 5 each), CH-157MN (n = 4 each)), and NF2wt (IOMM-Lee (n = 4 each), SAM (n = 5 each)) meningioma cell lines upon CRISPR-Cas9-mediated inactivation of either CD8A (control) or combined inactivation of YAP1 and TAZ (WWTR1). Error bars show SEM. Analysis was done using a two-tailed t test (A) or ordinary two-way ANOVA (B, for the last time point).

Figure 2: TEADi shows significant efficacy against benign and a subset of high-grade NF2 mutant meningioma cell lines. A) Cell viability dose response curves of 21 meningioma cell lines treated with different doses of four TEAD inhibitors (IAG-933, MYF-03-176, GNE-7883, K-975). Cell viability was measured upon the DMSO control reaching a confluence of > 80%. All experiments were performed in triplicates. B) Viability dose response curves of benign NF2mut (BenMen1, BrMen), aggressive high-grade NF2mut (KT21-MG1, CH-157MN), and NF2wt (IOMM-Lee, SAM) meningioma cell lines treated with different doses of four TEAD inhibitors (IAG-933, MYF-03-176, GNE-7883, K-975). All experiments were performed in triplicates. C) Growth curves measured by live-cell imaging of benign NF2mut (BenMen1, BrMen), aggressive high-grade NF2mut (KT21-MG1, CH-157MN), and NF2wt (IOMM-Lee, SAM) meningioma cell lines treated with different doses of the TEAD inhibitor IAG-933 (100, 200, 500, 1000 nM, 0.05% DMSO). All experiments were performed in triplicates. D) Expression of the YAP1/TAZ-TEAD target gene CTGF in benign NF2mut (BenMen1, BrMen), aggressive high-grade NF2mut (KT21-MG1, CH-157MN), and NF2wt (IOMM-Lee, SAM) meningioma cell lines upon treatment with four TEAD inhibitors (IAG-933 (500 nM), MYF-03-176 (500 nM), GNE-7883 (5000 nM), K-975 (1000 nM)). All experiments were performed in triplicates. Error bars show SD (A, B) or SEM (D). Analysis was done using an ordinary one-way ANOVA (D) or ordinary two-way ANOVA (A, B, comparison at 200 nM) with multiple comparisons testing.

Figure 3: TEADi treatment results in a downregulation of YAP1/TAZ-TEAD signaling in both TEADi-sensitive and -resistant cell lines. A) PCA plot with RNA-Seq data of DMSO-treated samples of benign NF2mut (BenMen1, BrMen), aggressive high-grade NF2mut (KT21-MG1,

CH-157MN), and NF2wt (IOMM-Lee, SAM) meningioma cell lines (n = 3 each). B) PCA plot showing DMSO, IAG-933, or MYF-03-176-treated samples of the same six meningioma lines (n = 3 each). C) PCA plots showing DMSO, IAG-933, or MYF-03-176-treated samples of benign NF2mut (BenMen1, left), high-grade NF2mut (CH-157MN, middle), or NF2wt (IOMM-Lee, right panel) meningioma cell lines. D) Hierarchical clustering of all six cell lines shows clustering along the lines of NF2 status and TEADi-sensitivity/resistance. E) Volcano plot showing differentially expressed genes between BenMen1 cells treated with DMSO vs TEADi (IAG-933). Yellow dots represent known YAP1/TAZ-TEAD target genes. F) Heatmap showing expression of significantly regulated genes in DMSO, IAG-933, and MYF-03-176-treated BenMen1 meningioma cells.

Figure 4: TEADi induces MEK-ERK and mTOR-S6 (but not PI3K-AKT) signaling in TEADi-resistant cell lines. A) Representative western blots showing phosphorylated and total protein levels of AKT, ERK, and S6 in two TEADi-sensitive (KT21-MG1, ARC) and two TEADi-resistant (GAR, IOMM-Lee) meningioma cell lines upon treatment with either DMSO (control) or TEADi (IAG-933 or MYF-03-176, 500 nM each). Actin was used as a loading control.

Figure 5: Co-targeting MAPK, mTOR-S6, or FAK signaling is able to overcome resistance to TEADi. A-B) Growth curves (A) and end point viability (B) of TEADi-sensitive or -resistant meningioma cell lines upon co-treatment with combinations of TEADi (IAG-933, 200 nM (sensitive lines) or 500 nM (resistant lines)), PI3Ki (pictilisib, 50 nM), MEKi (trametinib), or mTORi (torin-2). All experiments were performed in triplicates. C) Synergy plots for TEADi/MEKi or TEADi/mTORi combination treatments of TEADi-sensitive (KT21-MG1) or -resistant (IOMM-Lee) meningioma cell lines. D) Western Blot showing activation of MAPK (p-ERK), PI3K-AKT (p-AKT), or mTOR-S6 (p-S6) pathways in TEADi-resistant IOMM-Lee cells upon treatment with TEADi (IAG-933), MEKi (trametinib), mTORi (torin-2), or PI3Ki (pictilisib) in various combinations. Actin was used as a loading control. E) Growth curves of TEADi-resistant CH-157MN cells upon treatment with TEADi (IAG-933, 200 nM) or additional mTOR inhibitors (torin-2, rapamycin, vistusertib, everolimus, sapanisertib, 10 nM each). All experiments were performed in triplicates. F) End point viability of TEADi-sensitive and -resistant cell lines upon treatment with TEADi (IAG-933, 200 nM) or FAKi (TAE226, 500 nM). Error bars show SEM (A, B, E, F). Analysis was done using an ordinary one-way ANOVA (B,F) or ordinary two-way ANOVA (A, E, comparison at last time point) with multiple comparisons testing. Synergy analysis for two-way treatments was done with SynergyFinder3.0.

Supplementary Tables:

Suppl. Table S1: Enrichment of YAP1/TAZ-TEAD target genes in the differentially regulated genes identified in the six meningioma cell lines upon IAG-933 or MYF-03-176 treatment by RNA-Seq

Suppl. Table S2: Significantly enriched KEGG terms in the six meningioma cell lines upon IAG-933 treatment

Suppl. Table S3: Supplementary methods. A) Antibodies used B) sgRNA sequences C) Primers.

References

1. Szulzewsky F, Thirimanne HN, Holland EC. Meningioma: current updates on genetics, classification, and mouse modeling. *Ups J Med Sci.* 2024; 129.
2. Ostrom QT, Price M, Neff C, et al. CBTRUS Statistical Report: Primary Brain and Other Central Nervous System Tumors Diagnosed in the United States in 2016-2020. *Neuro Oncol.* 2023; 25(12 Suppl 2):iv1–iv99.
3. Ogasawara C, Philbrick BD, Adamson DC. Meningioma: A Review of Epidemiology, Pathology, Diagnosis, Treatment, and Future Directions. *Biomedicines.* 2021; 9(3).
4. Depond CC, Zouaoui S, Darlix A, et al. Descriptive epidemiology of 30,223 histopathologically confirmed meningiomas in France: 2006-2015. *Acta Neurochir (Wien).* 2024; 166(1):214.
5. Kshettry VR, Ostrom QT, Kruchko C, Al-Mefty O, Barnett GH, Barnholtz-Sloan JS. Descriptive epidemiology of World Health Organization grades II and III intracranial meningiomas in the United States. *Neuro Oncol.* 2015; 17(8):1166–1173.
6. Millward CP, Keshwara S, Islim AI, Zakaria R, Jenkinson MD. Clinical Presentation and Prognosis. *Adv Exp Med Biol.* 2023; 1416:5–20.
7. Westphal M, Saladino A, Tatagiba M. Skull Base Meningiomas. *Adv Exp Med Biol.* 2023; 1416:47–68.
8. Wen PY, Quant E, Drappatz J, Beroukhim R, Norden AD. Medical therapies for meningiomas. *J Neurooncol.* 2010; 99(3):365–378.
9. Chamberlain MC, Tsao-Wei DD, Groshen S. Temozolomide for treatment-resistant recurrent meningioma. *Neurology.* 2004; 62(7):1210–1212.
10. Chamberlain MC, Tsao-Wei DD, Groshen S. Salvage chemotherapy with CPT-11 for recurrent meningioma. *J Neurooncol.* 2006; 78(3):271–276.
11. Ji Y, Rankin C, Grunberg S, et al. Double-Blind Phase III Randomized Trial of the Antiprogestin Agent Mifepristone in the Treatment of Unresectable Meningioma: SWOG S9005. *J Clin Oncol.* 2015; 33(34):4093–4098.
12. Norden AD, Ligon KL, Hammond SN, et al. Phase II study of monthly pasireotide LAR (SOM230C) for recurrent or progressive meningioma. *Neurology.* 2015; 84(3):280–286.
13. Nassiri F, Liu J, Patil V, et al. A clinically applicable integrative molecular classification of meningiomas. *Nature.* 2021; 597(7874):119–125.
14. Sahm F, Schrimpf D, Stichel D, et al. DNA methylation-based classification and grading system for meningioma: a multicentre, retrospective analysis. *Lancet Oncol.* 2017; 18(5):682–694.
15. Brastianos PK, Twohy EL, Gerstner ER, et al. Alliance A071401: Phase II Trial of Focal Adhesion Kinase Inhibition in Meningiomas With Somatic NF2 Mutations. *J Clin Oncol.* 2023; 41(3):618–628.
16. Wen PY, Yung WK, Lamborn KR, et al. Phase II study of imatinib mesylate for recurrent meningiomas (North American Brain Tumor Consortium study 01-08). *Neuro Oncol.* 2009; 11(6):853–860.
17. Danish H, Brastianos P. Novel Medical Therapies in Meningiomas. *Adv Exp Med Biol.* 2023; 1416:213–223.
18. Choudhury A, Magill ST, Eaton CD, et al. Meningioma DNA methylation groups identify biological drivers and therapeutic vulnerabilities. *Nat Genet.* 2022; 54(5):649–659.
19. Thirimanne HN, Almiron-Bonnin D, Nuechterlein N, et al. Meningioma transcriptomic landscape demonstrates novel subtypes with regional associated biology and patient outcome. *Cell Genom.* 2024; 4(6):100566.

20. Clark VE, Erson-Omay EZ, Serin A, et al. Genomic analysis of non-NF2 meningiomas reveals mutations in TRAF7, KLF4, AKT1, and SMO. *Science.* 2013; 339(6123):1077–1080.
21. Sievers P, Arora S, Hielscher T, et al. Molecular signatures define BAP1-altered meningioma as a distinct CNS tumor with deregulation of Polycomb repressive complex target genes. *Neuro Oncol.* 2025; 27(9):2326–2340.
22. Gutmann DH, Giordano MJ, Fishback AS, Guha A. Loss of merlin expression in sporadic meningiomas, ependymomas and schwannomas. *Neurology.* 1997; 49(1):267–270.
23. Smith MJ. Germline and somatic mutations in meningiomas. *Cancer Genet.* 2015; 208(4):107–114.
24. Huang J, Wu S, Barrera J, Matthews K, Pan D. The Hippo signaling pathway coordinately regulates cell proliferation and apoptosis by inactivating Yorkie, the Drosophila Homolog of YAP. *Cell.* 2005; 122(3):421–434.
25. Zhang N, Bai H, David KK, et al. The Merlin/NF2 tumor suppressor functions through the YAP oncoprotein to regulate tissue homeostasis in mammals. *Dev Cell.* 2010; 19(1):27–38.
26. Yin F, Yu J, Zheng Y, Chen Q, Zhang N, Pan D. Spatial organization of Hippo signaling at the plasma membrane mediated by the tumor suppressor Merlin/NF2. *Cell.* 2013; 154(6):1342–1355.
27. Meng Z, Moroishi T, Guan KL. Mechanisms of Hippo pathway regulation. *Genes Dev.* 2016; 30(1):1–17.
28. Szulzewsky F, Holland EC, Vasioukhin V. YAP1 and its fusion proteins in cancer initiation, progression and therapeutic resistance. *Dev Biol.* 2021; 475:205–221.
29. Baia GS, Caballero OL, Orr BA, et al. Yes-associated protein 1 is activated and functions as an oncogene in meningiomas. *Mol Cancer Res.* 2012; 10(7):904–913.
30. Parrish AG, Arora S, Thirimanne HN, et al. Aggressive high-grade NF2 mutant meningiomas downregulate oncogenic YAP signaling via the upregulation of VGLL4 and FAT3/4. *Neuro-Oncology Advances.* 2024(vdae148).
31. Striedinger K, VandenBerg SR, Baia GS, McDermott MW, Gutmann DH, Lal A. The neurofibromatosis 2 tumor suppressor gene product, merlin, regulates human meningioma cell growth by signaling through YAP. *Neoplasia.* 2008; 10(11):1204–1212.
32. Szulzewsky F, Arora S, Arakaki AKS, et al. Both YAP1-MAML2 and constitutively active YAP1 drive the formation of tumors that resemble NF2 mutant meningiomas in mice. *Genes Dev.* 2022; 36(13-14):857–870.
33. Sievers P, Chiang J, Schrimpf D, et al. YAP1-fusions in pediatric NF2-wildtype meningioma. *Acta Neuropathol.* 2020; 139(1):215–218.
34. Szulzewsky F, Arora S, Hoellerbauer P, et al. Comparison of tumor-associated YAP1 fusions identifies a recurrent set of functions critical for oncogenesis. *Genes Dev.* 2020; 34(15-16):1051–1064.
35. Parrish AG, Thirimanne HN, Arora S, et al. PTEN deficiency linked to chromosome 10q loss leads to aggressive NF2 mutant meningioma biology. *bioRxiv.* 2025.
36. Landry AP, Wang JZ, Patil V, et al. Chromosome 1p Loss and 1q Gain for Grading of Meningioma. *JAMA Oncol.* 2025; 11(6):644–649.
37. Pobbati AV, Kumar R, Rubin BP, Hong W. Therapeutic targeting of TEAD transcription factors in cancer. *Trends Biochem Sci.* 2023; 48(5):450–462.
38. Chapeau EA, Sansregret L, Galli GG, et al. Direct and selective pharmacological disruption of the YAP-TEAD interface by IAG933 inhibits Hippo-dependent and RAS-MAPK-altered cancers. *Nat Cancer.* 2024; 5(7):1102–1120.
39. Paul S, Hagenbeek TJ, Tremblay J, et al. Cooperation between the Hippo and MAPK pathway activation drives acquired resistance to TEAD inhibition. *Nat Commun.* 2025; 16(1):1743.

40. Lu W, Fan M, Ji W, et al. Structure-Based Design of Y-Shaped Covalent TEAD Inhibitors. *J Med Chem.* 2023; 66(7):4617–4632.
41. Kaneda A, Seike T, Danjo T, et al. The novel potent TEAD inhibitor, K-975, inhibits YAP1/TAZ-TEAD protein-protein interactions and exerts an anti-tumor effect on malignant pleural mesothelioma. *Am J Cancer Res.* 2020; 10(12):4399–4415.
42. Yap TA, Kwiatkowski DJ, Dagogo-Jack I, et al. YAP/TEAD inhibitor VT3989 in solid tumors: a phase 1/2 trial. *Nat Med.* 2025; 31(12):4281–4290.
43. Liu Q, Xu C, Kirubakaran S, et al. Characterization of Torin2, an ATP-competitive inhibitor of mTOR, ATM, and ATR. *Cancer Res.* 2013; 73(8):2574–2586.
44. Carriere A, Romeo Y, Acosta-Jaquez HA, et al. ERK1/2 phosphorylate Raptor to promote Ras-dependent activation of mTOR complex 1 (mTORC1). *J Biol Chem.* 2011; 286(1):567–577.
45. Ma L, Chen Z, Erdjument-Bromage H, Tempst P, Pandolfi PP. Phosphorylation and functional inactivation of TSC2 by Erk implications for tuberous sclerosis and cancer pathogenesis. *Cell.* 2005; 121(2):179–193.
46. Akao K, Sato T, Mishiro-Sato E, et al. TEAD-independent cell growth of Hippo-inactive mesothelioma cells: Unveiling resistance to TEAD inhibitor K-975 through MYC signaling activation. *Mol Cancer Ther.* 2024.
47. Kulkarni A, Mohan V, Tang TT, et al. Identification of resistance mechanisms to small-molecule inhibition of TEAD-regulated transcription. *EMBO Rep.* 2024; 25(9):3944–3969.
48. Moure CJ, Vara B, Cheng MM, et al. Activation of Hepatocyte Growth Factor/MET Signaling as a Mechanism of Acquired Resistance to a Novel YAP1/TEAD Small Molecule Inhibitor. *Mol Cancer Ther.* 2024; 23(8):1095–1108.
49. Garralda E, Florescu M, Aerts JG, et al. 919O - A first-in-human study of oral IAG933 in adult patients with advanced mesothelioma and other solid tumours. *ESMO Congress* 2025.
50. Paul S, Sims J, Pham T, Dey A. Targeting the Hippo pathway in cancer: kidney toxicity as a class effect of TEAD inhibitors? *Trends Cancer.* 2025; 11(1):25–36.
51. Ragel BT, Couldwell WT, Gillespie DL, Wendland MM, Whang K, Jensen RL. A comparison of the cell lines used in meningioma research. *Surg Neurol.* 2008; 70(3):295–307; discussion 307.
52. Ianevski A, Giri AK, Aittokallio T. SynergyFinder 3.0: an interactive analysis and consensus interpretation of multi-drug synergies across multiple samples. *Nucleic Acids Res.* 2022; 50(W1):W739–W743.
53. Hoellerbauer P, Kufeld M, Paddison PJ. Efficient Multi-Allelic Genome Editing of Primary Cell Cultures via CRISPR-Cas9 Ribonucleoprotein Nucleofection. *Curr Protoc Stem Cell Biol.* 2020; 54(1):e126.

Table 2 - Overview of different meningioma cell lines tested.

	IAG-933	**MYF-03-176**	**GNE-7883**	**K-975**	**NF2 status**	**WHO grade**
BenMen1	78	76	410	2443	NF2 MUT	WHO I
BrMen	39	456	1629	>5000	NF2 MUT	WHO I
GRA	66	495	4989	>5000	NF2 MUT	WHO I
Patient 13	111	434	181	665	NF2 MUT	WHO I

Patient 16	170	3981	>5000	>5000	NF2 MUT	WHO I
Patient 5	187	1479	4797	>5000	NF2 MUT	WHO II
Patient 17	210	1148	4498	>5000	NF2 MUT	WHO II
KT21-MG1	108	139	713	4236	NF2 MUT	WHO III
CH-157MN	273	>5000	2582	>5000	NF2 MUT	WHO III
Pro	220	457	2113	3459	NF2 MUT	n/a
Patient 6	1503	>5000	>5000	>5000	NF2 WT	WHO I
Patient 12	1199	>5000	>5000	>5000	NF2 WT	WHO I
SAM	454	>5000	>5000	>5000	NF2 WT	WHO I
GAB	286	>5000	3899	>5000	NF2 WT	WHO I
GAR	479	>5000	>5000	>5000	NF2 WT	WHO I
IOMM-Lee	351	>5000	>5000	>5000	NF2 WT	WHO III
MUL	56	101	499	1936	n/a	WHO I
NOR	131	500	453	4966	n/a	WHO I
FAS	77	352	334	444	n/a	WHO I
ARC	51	257	1005	2148	n/a	WHO I
Patient 8	673	>5000	>5000	>5000	n/a	WHO I
Patient 9	661	3475	>5000	>5000	n/a	WHO I

Figure 1

A Expression of the YAP1/TAZ-TEAD target gene CTGF upon CRISPR-Cas9-mediated inactivation of YAP1 and TAZ

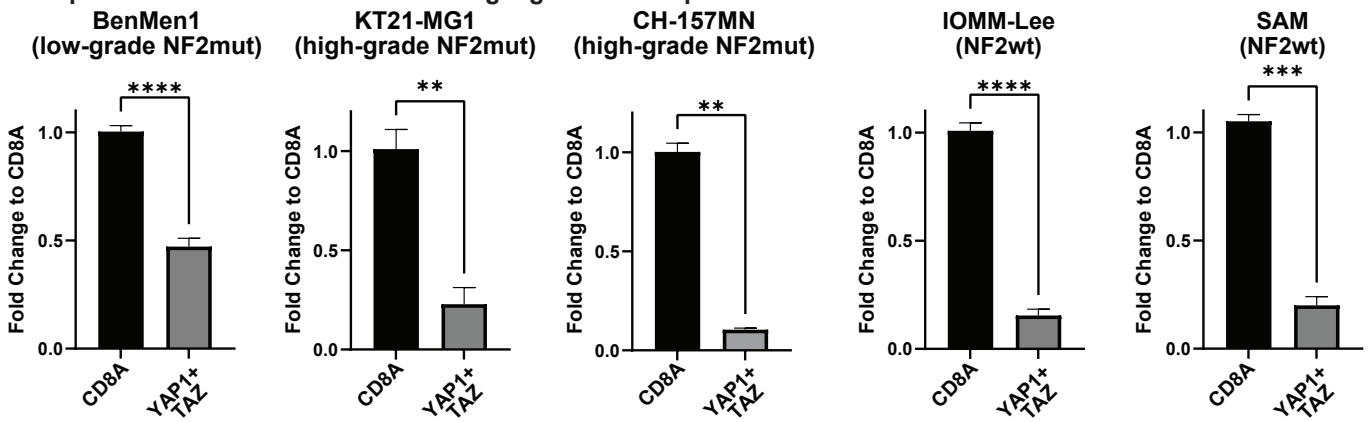

B Growth curves of five meningioma cell lines upon CRISPR-Cas9-mediated inactivation of YAP1 and TAZ

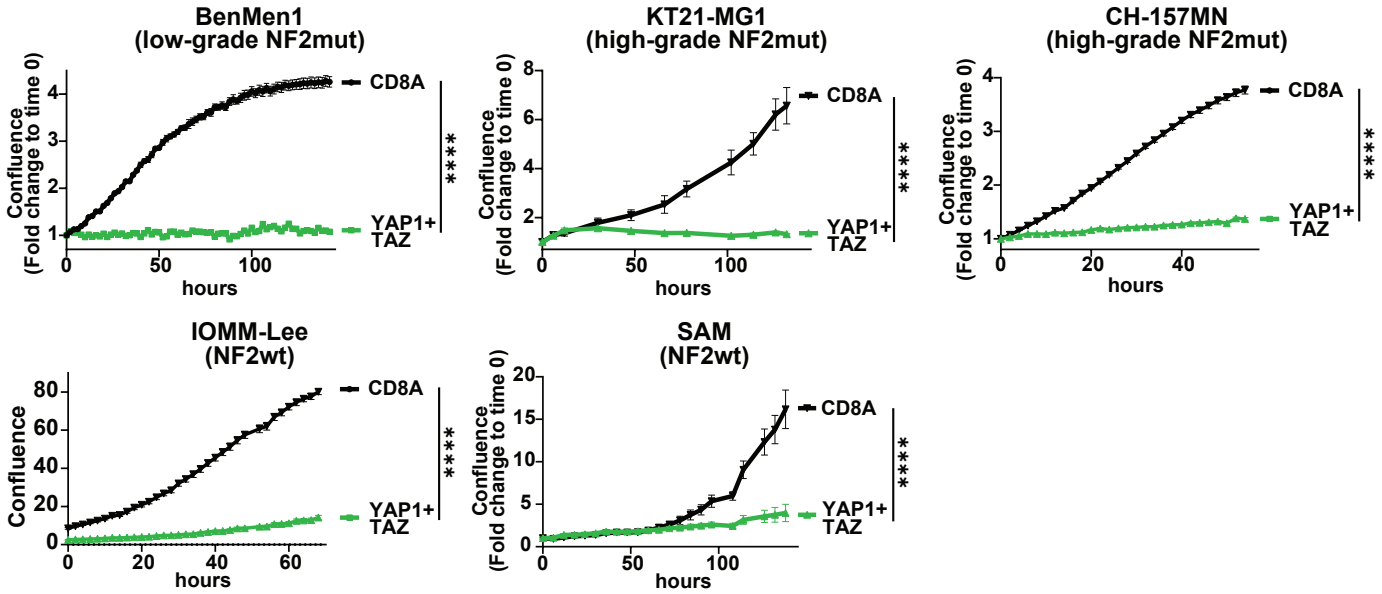

Figure 2

A Dose-response curves of 21 meningioma cell lines treated with four different TEAD inhibitors

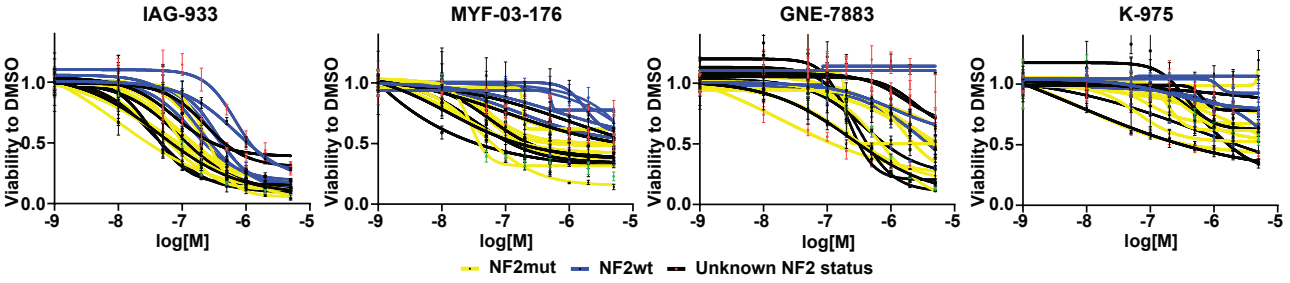

B Dose-response curves of six meningioma cell lines treated with four different TEAD inhibitors

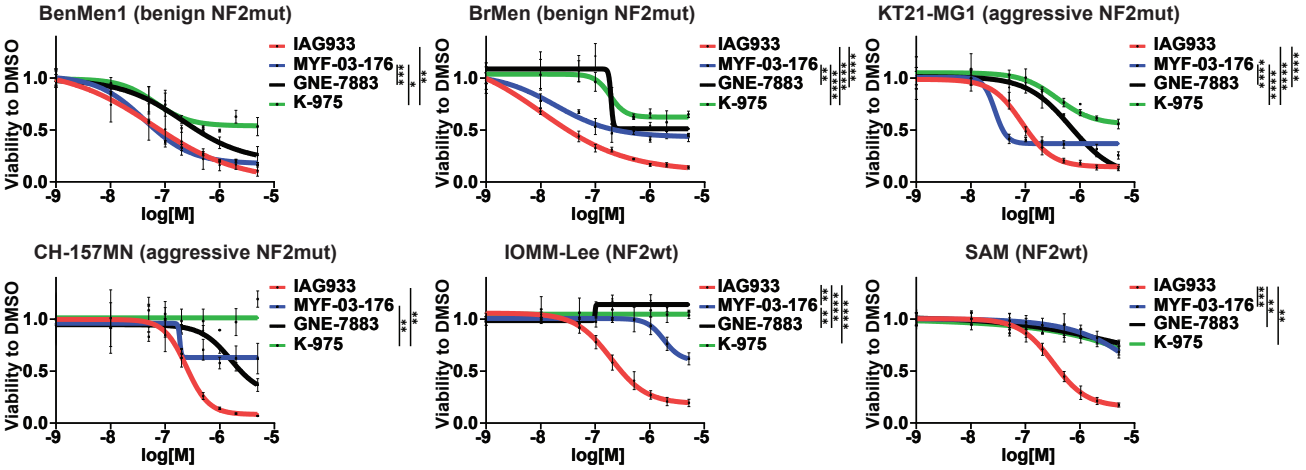

C Growth curves of six meningioma cell lines treated with the TEAD inhibitor IAG-933

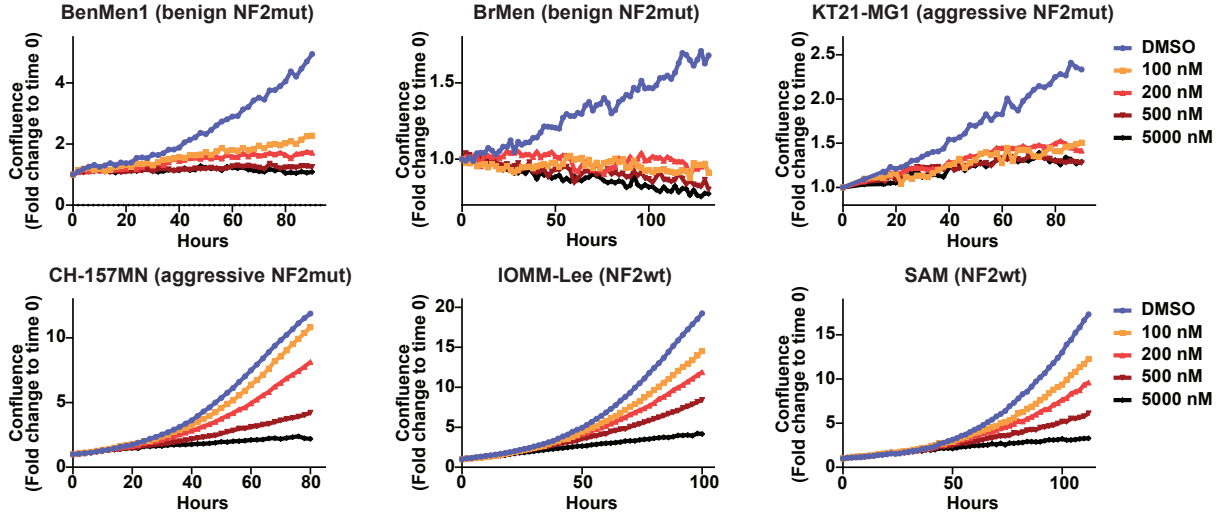

D Expression of the YAP1/TAZ-TEAD target gene CTGF TEADi treatment with four different TEAD inhibitors

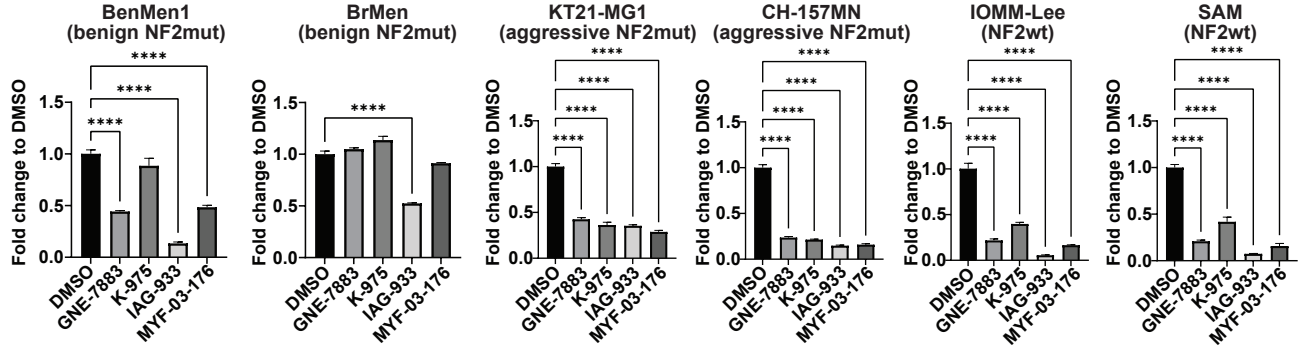

Figure 3

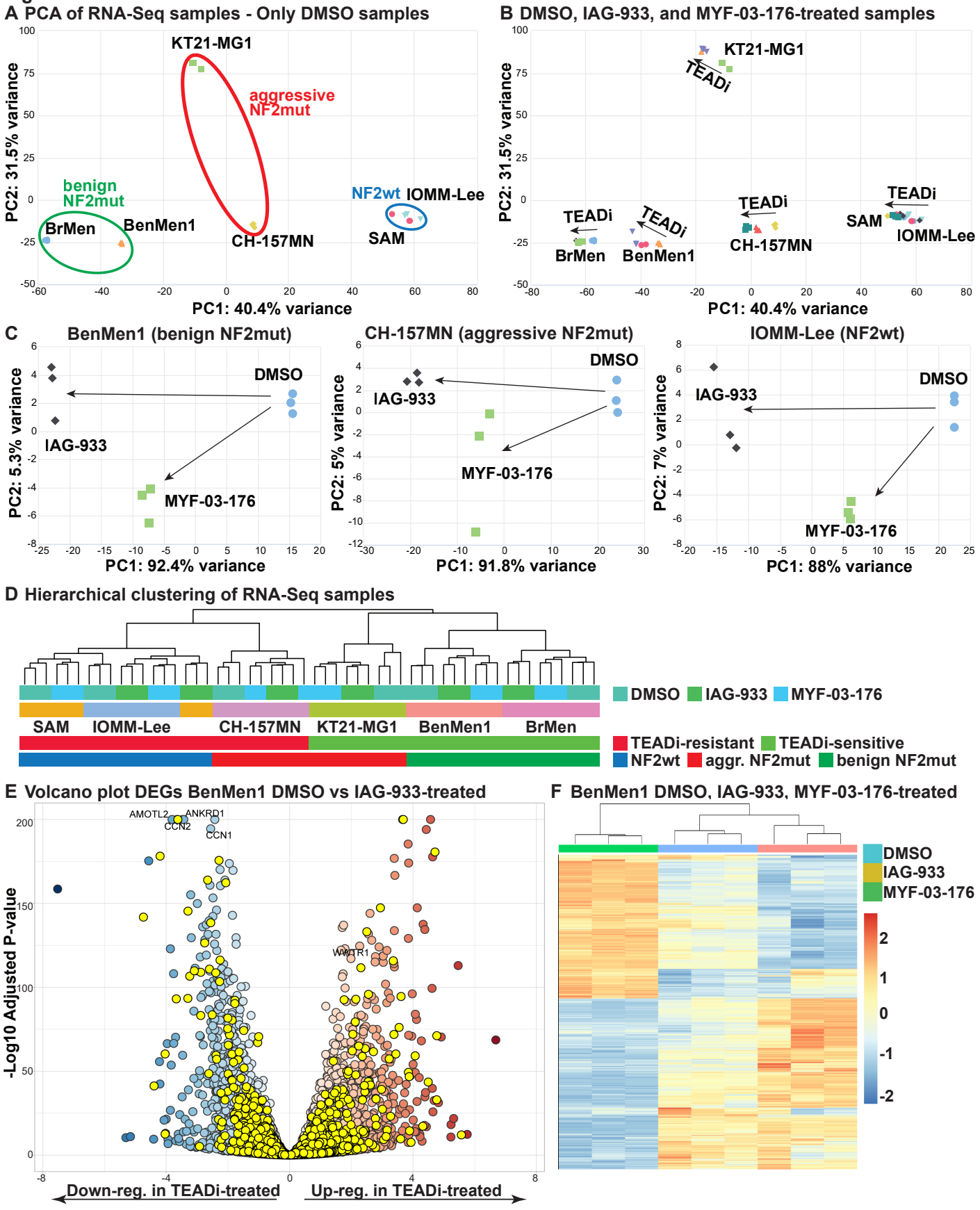
A PCA of RNA-Seq samples - Only DMSO samples
KT21-MG1
aggressive NF2mut
benign NF2mut
BrMen
BenMen1
CH-157MN
NF2wt
IOMM-Lee
SAM
PC2: 31.5% variance
PC1: 40.4% variance
B DMSO, IAG-933, and MYF-03-176-treated samples
KT21-MG1
TEADi
TEADi
TEADi
TEADi
TEADi
BrMen
BenMen1
CH-157MN
SAM
IOMM-Lee
PC2: 31.5% variance
PC1: 40.4% variance
C
BenMen1 (benign NF2mut)
DMSO
IAG-933
MYF-03-176
PC2: 5.3% variance
PC1: 92.4% variance
CH-157MN (aggressive NF2mut)
DMSO
IAG-933
MYF-03-176
PC2: 5% variance
PC1: 91.8% variance
IOMM-Lee (NF2wt)
DMSO
IAG-933
MYF-03-176
PC2: 7% variance
PC1: 88% variance
D Hierarchical clustering of RNA-Seq samples
DMSO
IAG-933
MYF-03-176
SAM
IOMM-Lee
CH-157MN
KT21-MG1
BenMen1
BrMen
TEADi-resistant
TEADi-sensitive
NF2wt
aggr. NF2mut
benign NF2mut
E Volcano plot DEGs BenMen1 DMSO vs IAG-933-treated
AMOTL2
ANKRD1
CCN2
CCN1
WWTR1
-Log10 Adjusted P-value
Down-reg. in TEADi-treated
Up-reg. in TEADi-treated
F BenMen1 DMSO, IAG-933, MYF-03-176-treated
DMSO
IAG-933
MYF-03-176

Figure 4

A Activation of MAPK, PI3K-AKT-mTOR pathways in sensitive and resistant lines upon TEADi treatment

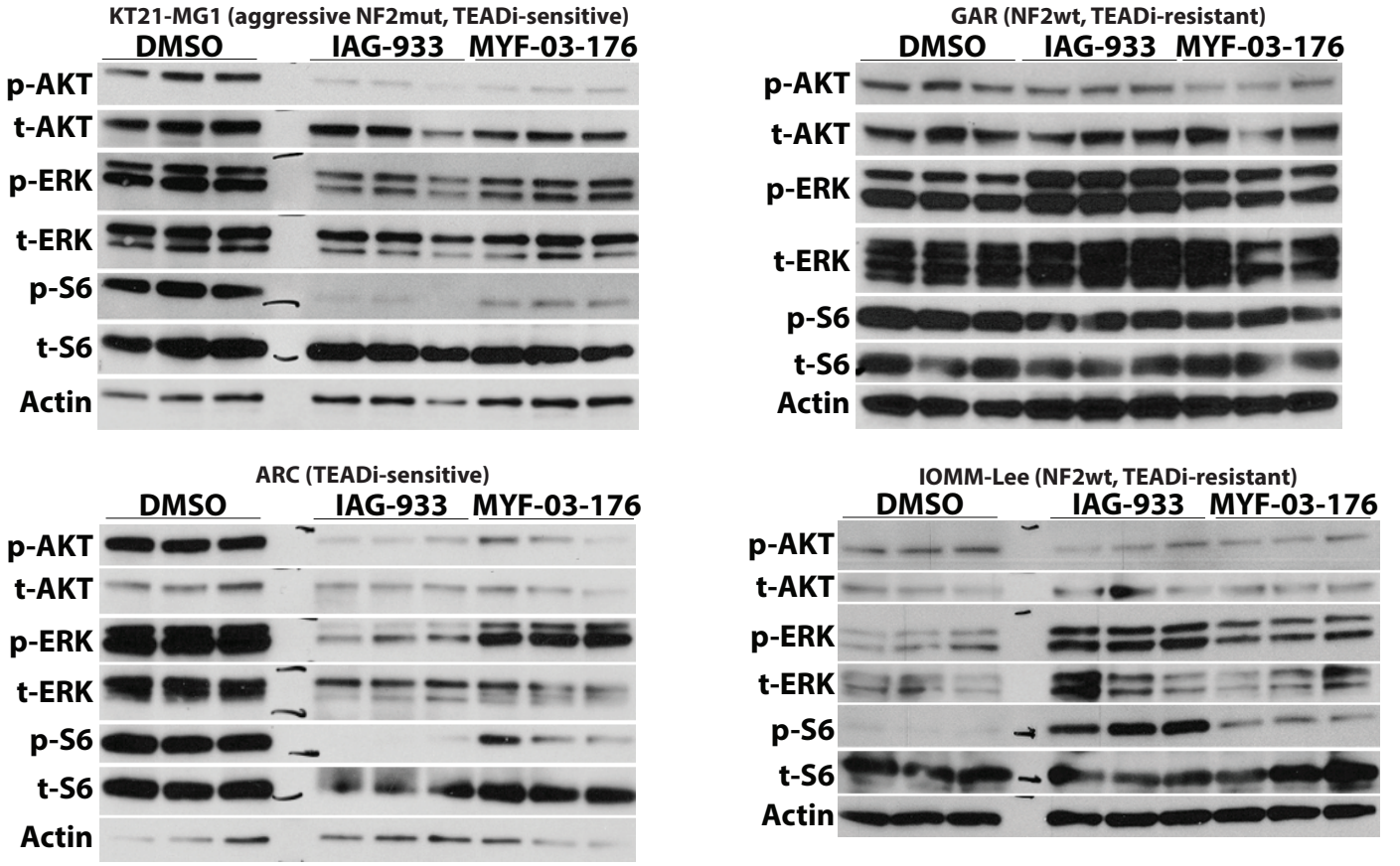

Figure 5

A Growth curves of sensitive and resistant cell lines cotreated with TEADi and MEKi/mTORi

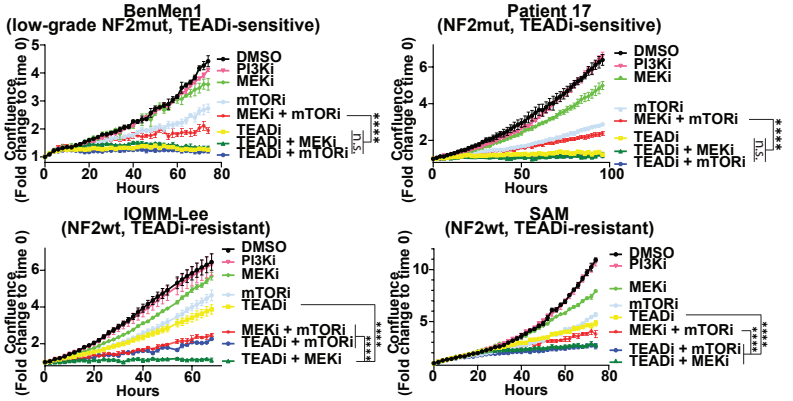

B Viability of sensitive and resistant cell lines cotreated with TEADi and MEKi/mTORi

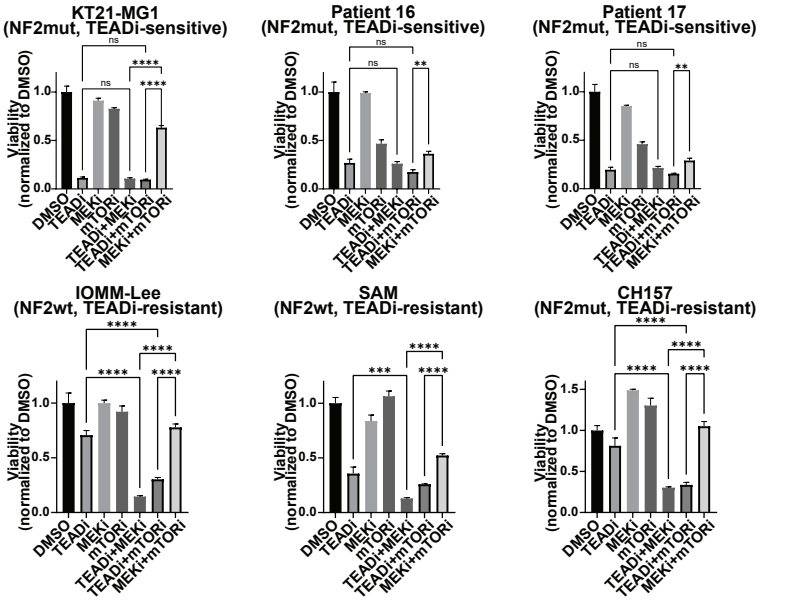

C Synergy plots of sensitive and resistant cell lines cotreated with TEADi and MEKi/mTORi

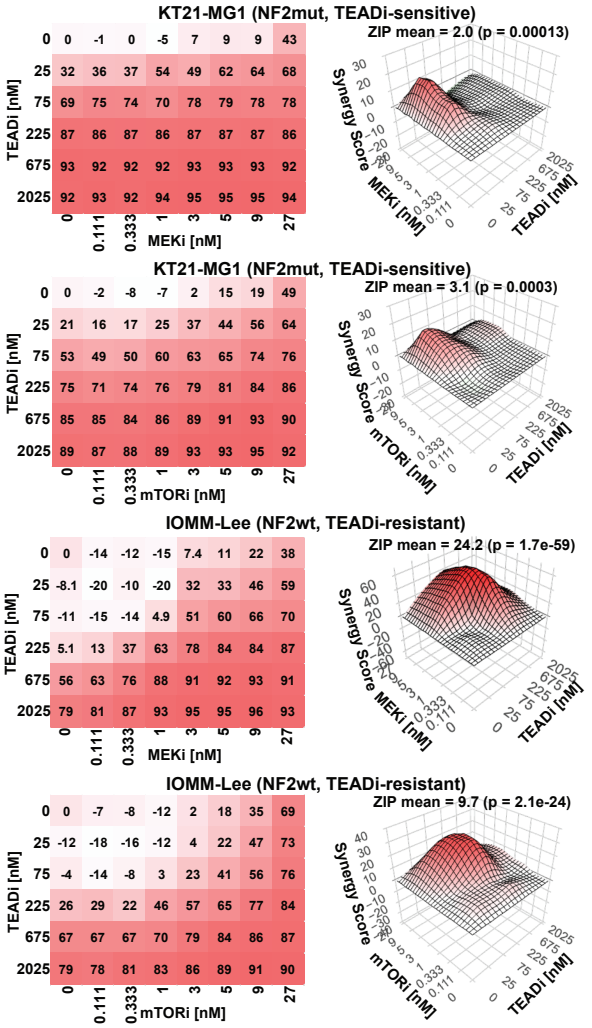

D Cotreatment with TEADi and MEKi/mTORi

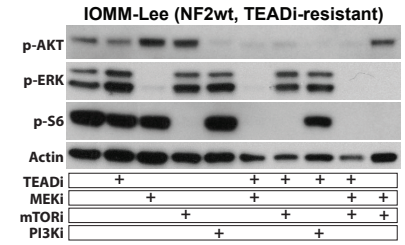

E Cotreatment with TEADi and FDA-approved mTORi

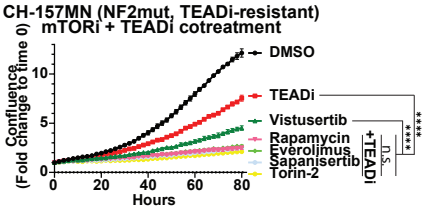
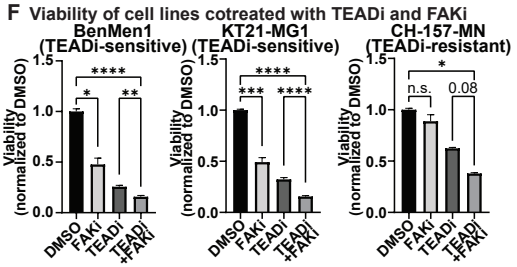
F Viability of cell lines cotreated with TEADi and FAKi